RSC Medicinal Chemistry

ROYAL SOCIETY OF CHEMISTRY

RESEARCH ARTICLE

View Article Online
View Journal | View Issue

Cite this: *RSC Med. Chem.*, 2021, **12**, 970

Design, synthesis, crystal structure and anti-plasmodial evaluation of tetrahydrobenzo[4,5]thieno[2,3-*d*]pyrimidine derivatives†

Kavita Pal,[a] Md Kausar Raza,[b] Jenny Legac,[c] Md. Ataur Rahman,[d] Shoaib Manzoor,[a] Philip J. Rosenthal[c] and Nasimul Hoda *[a]

Effective chemotherapy is essential for controlling malaria. However, resistance of *Plasmodium falciparum* to existing antimalarial drugs has undermined attempts to control and eventually eradicate the disease. In this study, a series of 2-((substituted)(4-(5,6,7,8-tetrahydrobenzo[4,5]thieno[2,3-*d*]pyrimidin-4-yl)piperazin-1-yl)methyl)-6-substitutedphenol derivatives were prepared using Petasis reaction with a view to evaluate their activities against *P. falciparum*. The development of synthesized compounds (**F1–F16**) was justified through the study of H^1 NMR, C^{13} NMR, mass spectra. Compound **F1** and **F2** were also structurally validated by single crystal X-ray diffraction analysis. All the compounds were evaluated for their *in vitro* antiplasmodial assessment against the W2 strain (chloroquine-resistant) of *P. falciparum* IC_{50} values ranging from 0.74–6.4 μM. Two compounds, **F4** and **F16** exhibited significant activity against W2 strain of *P. falciparum* with 0.75 and 0.74 μM. The compounds (**F3–F6** and **F16**) were also evaluated for *in vitro* cytotoxicity against two cancer cell lines, human lung (A549) and cervical (HeLa) cells, which demonstrated non-cytotoxicity with significant selectivity indices. In addition, *in silico* ADME profiling and physiochemical properties predicts drug-like properties with a very low toxic effect. Thus, all these results indicate that tetrahydrobenzo[4,5]thieno[2,3-*d*]pyrimidine scaffolds may serve as models for the development of antimalarial agents.

Received 8th February 2021,
Accepted 26th April 2021

DOI: 10.1039/d1md00038a

rsc.li/medchem

1. Introduction

Malaria is a life-threatening parasitic infection and a major global health problem. The causative organism for the most virulent form of malaria, *Plasmodium falciparum*, accounts for significant worldwide health and socio-economic burdens.[1,2] In 2019, there were an estimated 229 million cases and 409 000 deaths from malaria.[3] Children aged less than five years are the most vulnerable group and accounted for 67% of all malaria deaths. The life cycle of malaria parasites includes multiple stages in the human host and mosquito vector.[4]

Chloroquine (CQ) was previously the first-line therapy for malaria[5–7] and it is still the drug of choice to treat uncomplicated malaria caused by *Plasmodium vivax* and other species,[8] but it is no longer used to treat *P. falciparum* malaria due to widespread resistance. CQ resistance has since spread to almost every part of the world and has necessitated the use of artemisinin-based combination therapy to treat falciparum malaria (ACT).[9] With ACT, the rapid-acting artemisinin component rapidly reduces parasite mass, and the longer-acting partner drug eliminates any remaining parasites.[10] However, the appearance of resistance to artemisinins in South-East Asia has led to failures of ACTs in Cambodia and surrounding countries and concerns regarding our ability to reliably treat malaria.[11–13] The emergence of resistance to artemisinins highlights the need for development of novel antimalarial drugs. The rapid and extensive rise of resistant mutants against frontline malaria treatments has led to their failures as a result, to rising concern over malaria eradication. Hence, this emergence of resistance is a reminder of the constant need for the development of novel antimalarial drugs with high efficacy, cost-effective and different mode of action to control and eventually abolish this parasitic disease. This resistance

[a] *Drug Design and Synthesis Laboratory, Department of chemistry, Jamia Millia Islamia, New Delhi 110025, India. E-mail: nhoda@jmi.ac.in; Fax: +91 11 26985507; Tel: +91 9910200655*
[b] *Department of Inorganic and Physical Chemistry, Indian Institute of Science, Bangalore 560012, India*
[c] *Department of Medicine, University of California, San Francisco, CA, USA*
[d] *Department of Chemistry and Chemical Biology, Harvard University, Cambridge, Massachusetts 02138, USA*

† Electronic supplementary information (ESI) available. CCDC 2008065 and 2008067. For ESI and crystallographic data in CIF or other electronic format see DOI: 10.1039/d1md00038a

phenomenon has accelerated the search for hybrid antimalarial to beat the matter of drug resistance.

The development of hybrid antimalarial agents involved the hybridisation of two different biologically active pharmacophores to produce a single hybrid antimalarial molecule with effective activity. Hybrids reduce the risk of drug resistance development by mutual protection of each pharmacophoric moiety.[14] Hybrid molecules have better solubility and lower toxicity than their free agents.[15] If the active moieties of the two partner drugs are connected through suitable space linker, then they may interact synergistically and exhibit higher activity than as individual agents.[16] It is easier to expect the pharmacokinetic properties of a hybrid and hence to manipulate than those of the two individual drugs. The problems relating to pharmacokinetics, metabolic stability, or side effects of individual molecules are better resolved in the form of a hybrid.[17] The hybrids were more effective than their bioactive constituents to kill resistant parasites because cells take up the active parts of both drugs simultaneously.[18]

Building on our interest in molecular hybridization to develop new antimalarials, we report here a rational design of a series of new 2-(phenyl(4-(5,6,7,8-tetrahydrobenzo[4,5]thieno[2,3-*d*]pyrimidin-4-yl)piperazin-1-yl)methyl)phenol derivatives as antimalarial agents based on different pharmacophore combination strategy (Fig. 1). The hit structures thienopyrimidine and diphenylmethylpiperazine scaffolds are found in various anti-parasitic agents with significant pharmacokinetic profiles. The preference of selecting thienopyrimidine hit structure was due to its versatile and broad biological properties. The thienopyrimidine derivatives showed extensive pharmacological properties including; anti-inflammatory,[19,20] anticancer,[21,22] antioxidant,[23] antimicrobial,[24] anti-tuberculosis[25] and antimalarial.[26,27] The 2,4-diaminothieno[2,3-*d*]pyrimidine derivatives have previously been reported against *P. berghei* and *P. gallinaceum*. The activity of these compounds was low and not significant but some compounds displayed significant activity at very high doses (640 mg kg^{-1}).[28,29] Hence, on the basis of this available bioassay data, we do not propose further investigation of these variants of the 2,4-diaminothieno[2,3-*d*]pyrimidine ring system. Among thieno[2,3-*d*]pyrimidine derivatives, the derivatives of tetrahydrobenzothieno[2,3-*d*]pyrimidine revealed potential activity against various parasitic diseases.[27,30–32] Compound **I** (Fig. 1) is a novel anti-malarial agent suitable for hit-to-lead chemistry. It showed good anti-plasmodial activity (IC_{50} = 0.15 μM), *in vitro* ADME properties and *in vivo* activity in the *P. berghei* mouse model.[33] Woodring *et al.* evaluated various substituted thienopyrimidine **II** (Fig. 1) against various parasitic diseases including malaria[27,31] (ED_{50} = 0.15 μM for W2 strain). The thieno[2,3-*d*]pyrimidines derivatives are also reported as well-known inhibitor of dihydrofolate reductase (DHFR)[34–36] which is key enzyme in the folate biosynthetic pathway and important antimalarial target. Clinical efficacy of well-known antifolate antimalarial drugs such as pyrimethamine and cycloguanil have been compromised by resistance arising through mutations at various sites on the enzyme. But this problem has been solved by researchers by designing and synthesis of hybrid inhibitors with both rigid and flexible side-chains in the same molecule.[37,38] A study by Zaidi *et al.* showed that thieno[2,3-*d*]pyrimidines bearing piperazine sulphonamides **III** (Fig. 1) possess good antiplasmodial activity and are active against the *Pf*DHFR

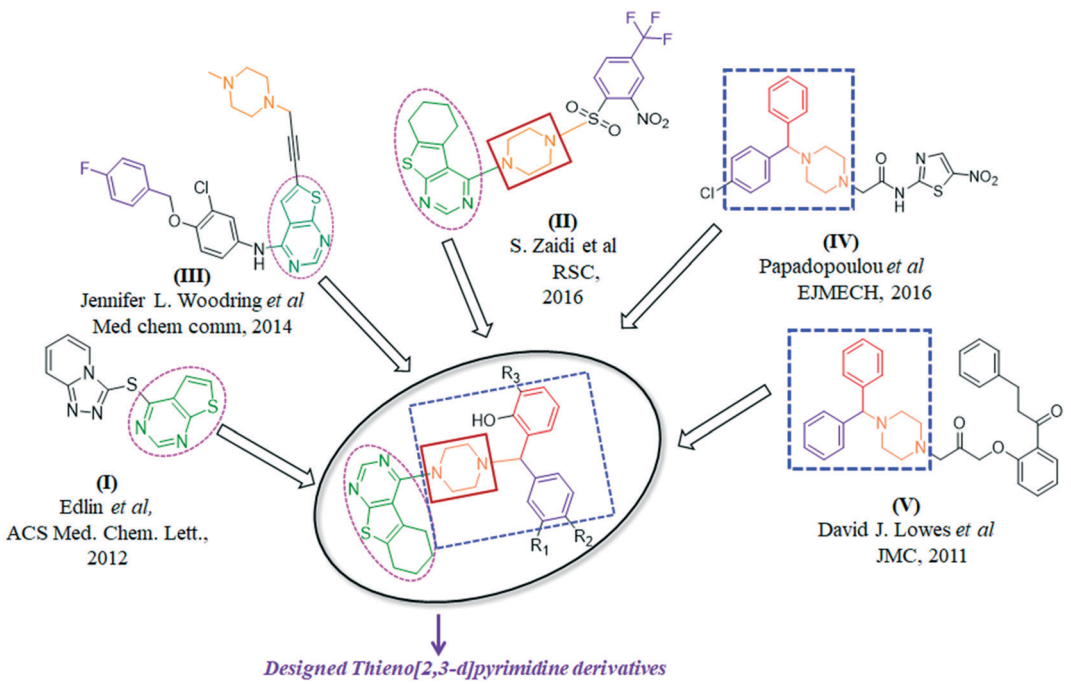

Fig. 1 Rationale for the design of substituted tetrahydrobenzothieno[2,3-*d*]pyrimidine derivatives.

enzyme[26] (IC_{50} = <0.1 μM). As represented in Fig. 1, the pharmacophore fragment, thienopyrimidine is conjugated with diphenyl derivatives through a linker piperazine. Compound **IV** (IC_{50} = 3.39 μM) & V (EC_{50} = 0.92 μM) contain diphenylmethylpiperazine pharmacophore which makes these compound most active against *P. falciparum* confirmed antiparasitic properties of diphenylmethylpiperazine.[39,40] Further, clotrimazole based antimalarials also confirmed the antimalarial potency of diphenylmethyl and triphenylmethyl pharmacophore.[41–43] The rationale behind the commencement of the piperazine ring in the current series of compounds can be easily identified on the basis of recent reports explaining the antimalarial enhancement with the introduction of the piperazine ring.[26,39,40,44]

By considering all these facts, we disclose the results of our efforts to synthesis series of new 2-(phenyl(4-(5,6,7,8-tetrahydrobenzo[4,5]thieno[2,3-*d*]pyrimidin-4-yl)piperazin-1-yl)methyl)phenol derivatives by using multicomponent Petasis reaction as the key step and their biological screening as antiplasmodial agents. The synthesized derivatives with significant antiplasmodial activity were evaluated for *in vitro* cytotoxicity screening. Furthermore, physicochemical and pharmacokinetics properties was predicted to determine the oral bioavailability of the leading candidates. Our results suggest the appropriateness of our newly synthesized compounds as models for further drug development.

2. Results and discussion

2.1. Synthetic chemistry

The development of the diversified substituted 2-(phenyl(4-(5,6,7,8-tetrahydrobenzo[4,5]thieno[2,3-*d*]pyrimidin-4-yl)piperazin-1-yl)methyl)phenol derivatives was accomplished *via* synthetic pathways shown in Scheme 1. The intermediate 2-amino-4,5,6,7-tetrahydrobenzo[*b*]thienophene-3-carboxylic acid ethyl ester compound **1** through Gewald reaction between cyclohexanone, elemental sulphur, ethyl cyanoacetate in ethanol in the presence of morpholine. The compound **1** was reacted with an excess formamide at 180 °C to obtain the cyclic pyrimidinone **2** compound.[45] To obtain compound **3**, compound **2** was refluxed in phosphorus oxychloride ($POCl_3$). Then compound **3** was reacted with anhydrous piperazine in methanol to obtain 4-(piperazin-1-yl)-5,6,7,8-tetrahydrobenzo[4,5]thieno[2,3-*d*]pyrimidine **4**. Finally, the target compounds (**F1–F16**) were obtained by the Petasis reaction between compound **4**, various substituted aromatic boronic acids and different substituted aldehydes (Table 1) in DMF at 90 °C. These compounds were purified by flash column chromatography and recrystallized from ethyl acetate. The compounds were stable in solid state at room temperature. The structures of these compounds were established through various analytical and spectroscopic techniques (^{1}H, ^{13}C NMR and mass spectra). The ^{1}H NMR showed common signals around 1.70, 1.76, 1.89, 1.90, 2.88 and 8.54 of the 4-piperazin-1-yl-5,6,7,8-tetrahydrobenzo[4,5]theino[2,3-*d*] pyrimidine fragments present in all the final compounds. The thienopyrimidine N–H was detected in a range of δ 8.54–8.50 as a singlet peak for all inhibitors. The aromatic O–H proton in all inhibitors occurred as a broad singlet in the range δ 11.70–11.05. The conversion of piperazine N–H to piperazine N–CH shifted the peak from a less de-shielded region δ 4–4.36 to a more de-shielded region δ 4.41–4.58. This result validates the formation of final compounds through the Petasis reaction. Protons of other aromatic substituents of the compounds were observed as expected. In a similar fashion common carbon peaks for tetrahydrobenzo[4,5]theino[2,3-*d*]pyrimidine fragments were observed in their respective positions in ^{13}C spectra. The peak for piperazine ring carbons was observed around 45 and 51 ppm. In all compounds, piperazine substituted alkylcarbon (N–CH) presented in the range δ 76.78–74.71 ppm. The carbon atoms of the aromatic substituents were

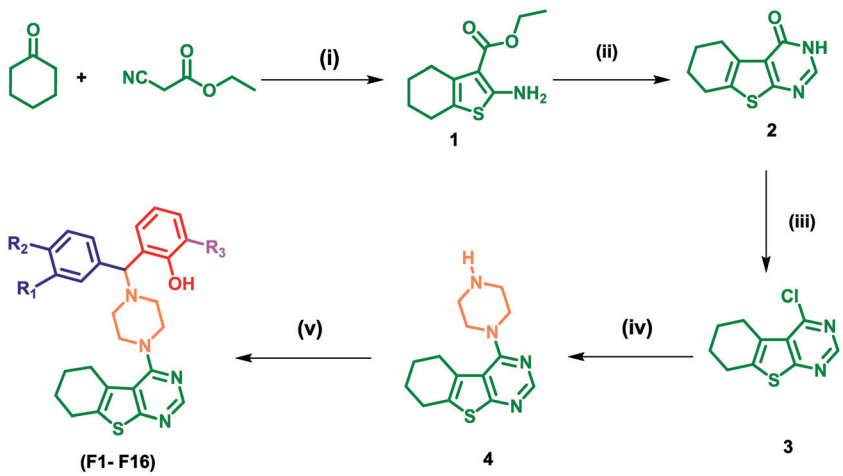

Scheme 1 Synthesis of 2-((subsituited)(4-(5,6,7,8-tetrahydrobenzo[4,5]thieno[2,3-*d*]pyrimidin-4-yl)piperazin-1-yl)methyl)phenol derivatives (**F1–F16**). Reagents and conditions: (i) morpholine, sulphur, absolute ethanol, 80 °C; (ii) formamide, 180 °C; (iii) $POCl_3$, TEA, 110 °C; (iv) piperazine, methanol, 70 °C; (v) salicylaldehyde or ortho vanillin, substituted boronic acid, DMF, 90 °C.

Table 1 Various substituents of 2-((subsituited)(4-(5,6,7,8-tetrahydrobenzo[4,5]thieno[2,3-*d*]pyrimidin-4-yl)piperazin-1-yl)methyl) phenol derivatives

Compounds	R_1	R_2	R_3	Compounds	R_1	R_2	R_3
F1	–H	$-OCH_3$	–H	**F9**	–H	$-OCH_3$	$-OCH_3$
F2	–H	$-CH_3$	–H	**F10**	–H	$-CH_3$	$-OCH_3$
F3	–F	–F	–H	**F11**	–F	–F	$-OCH_3$
F4	–Cl	–Cl	–H	**F12**	–Cl	–Cl	$-OCH_3$
F5	–H	$-OCF_3$	–H	**F13**	–H	$-OCF_3$	$-OCH_3$
F6	–Cl	–F	–H	**F14**	–Cl	–F	$-OCH_3$
F7	–H	–F	–H	**F15**	–H	–F	$-OCH_3$
F8	–H	$-CF_3$	–H	**F16**	–H	$-CF_3$	$-OCH_3$

found to be placed at the expected positions in the aromatic region. The HRMS spectra of compounds (**F1–F16**) also corroborated their proposed structures.

2.2. X-ray crystallography study

Compounds' structural integrity was further confirmed through single X-ray crystallography (Fig. 2, Table 2). **F1** crystallizes in triclinic in $P\bar{1}$ space group (Fig. 2a), whereas **F2** crystallizes in monoclinic of $P12_1/n1$ space group (Fig. 2b) crystal system respectively. The S(1)–C(6) and S(1)–C(1) bond distance in compounds **F1** is 1.745(8) and 1.747(8), whereas **F2** was found 1.7400(19) and 1.7282(19) Å respectively. The bond lengths of C(17)–OH in **F1** and **F2** were 1.356(9) and 1.365(2) Å, respectively (Table 3). The unit cell packing diagram of **F1** and **F2** reveals the H-bonding contacts between the phenolic group's hydrogen atoms with a nitrogen atom and the short contact bonding with their adjacent atoms (Fig. S49–S54, ESI†).

2.3. *In vitro* anti-plasmodial evaluation

The antiplasmodial activities of novel 16 synthesized 2-(phenyl(4-(5,6,7,8-tetrahydrobenzo[4,5]thieno[2,3-*d*]pyrimidin-4-yl)piperazin-1-yl)methyl)phenol derivatives was evaluated against the W2 strain of *P. falciparum* (Table 4) where Chloroquine (CQ) was used as the standard compound. As

Table 2 Crystal data and structure refinement for 2-((4-methoxyphenyl)(4-(5,6,7,8-tetrahydrobenzo[4,5]thieno[2,3-*d*]pyrimidin-4-yl)piperazin-1-yl)methyl)phenol (**F1**) and 2-((4-(5,6,7,8-tetrahydrobenzo[4,5]thieno[2,3-*d*]pyrimidin-4-yl)piperazin-1-yl)(p-tolyl)methyl)phenol (**F2**)

	F1	**F2**
Empirical formula	$C_{28}H_{31}N_4O_2S$	$C_{28}H_{31}N_4OS$
Formula weight	530.74	471.65
Crystal system	Triclinic	Monoclinic
Space group	$P\bar{1}$	$P12_1/n1$
a/Å	10.221(5)	13.815(4)
b/Å	13.970(9)	10.555(3)
c/Å	21.807(13)	17.808(5)
α/°	79.88(2)	90
β/°	76.458(13)	111.233(8)
γ/°	68.561(13)	90
V/Å^3	2804(3)	2420.3(12)
Z	4	4
T, K	296.15	296(2)
ρ_{calcd}/g cm^{-3}	1.2572	1.2943
λ/Å (Mo-Kα)	0.71073 Å	0.71073 Å
Data/restraints/param	18 309/0/694	7336/0/309
F(000)	1136.9259	1004.8513
GOF	1.0128	1.1189
$R(F_o)$,[a] $I > 2\sigma(I)$ [w$R(F_o)^b$]	0.1733 [0.3161]	0.0570 [0.1420]
R (all data) [wR (all data)]	0.5008 [0.4784]	0.0768 [0.1654]
Largest diff peak, hole (e Å^{-3})	2.3012, −2.0976	0.7938, −0.8371
$w = 1/[(\sigma F_o)^2 + (AP)^2 + (BP)]$	A = 0.173582	A = 0.064042
		B = 1.980359

[a] $R = \sum||F_o| - |F_c||/\sum|F_o|$. [b] $wR = \{\sum[w(F_o^2 - F_c^2)^2]/\sum[w(F_o)^2]\}^{1/2}$, where $P = (F_o^2 + 2F_c^2)/3$.

evident, although the tested compounds are not as active as standard drugs *viz.* CQ (0.17 μM), but most of the synthesized compounds exhibited good antiplasmodial activity showing range 0.74–6.40 μM. Investigation of the bioactivity data disclosed an interesting structure–activity relationships (SARs) among the set of tested compounds where activity varies with substitution on the aromatic rings. Nature of substituent present on both phenolic and benzene rings greatly affect the bioactivity result. Analysis of antiplasmodial activities of the synthesised compound revealed that those having substituent R_3 = H (**F1–F8**) on phenolic ring are more active than their

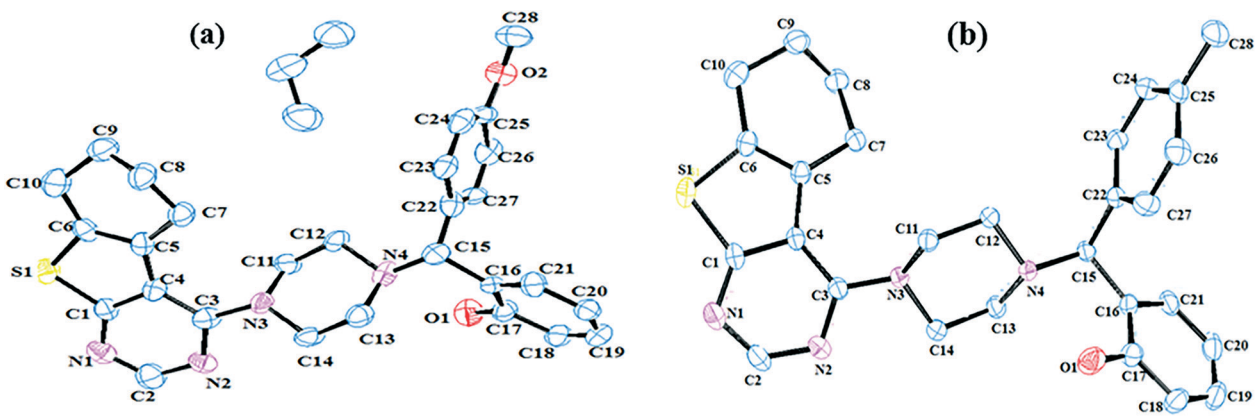

Fig. 2 ORTEP diagram of compounds **F1** (a) and **F2** (b) (50% probability level of thermal ellipsoids). Colour codes: carbon, blue; nitrogen, violet; sulphur, yellow and oxygen, red. Hydrogen atoms are omitted for clarity.

Table 3 Selected bond distance (Å) and bond angle (°) for compound **F1** and **F2** with estimated standard deviations in parentheses

	F1	F2
S(1)–C(6)	1.745(8)	1.7400(19)
S(1)–C(1)	1.747(8)	1.7282(19)
O(1)–C(17)	1.356(9)	1.365(2)
N(3)–C(3)	1.386(10)	1.392(2)
N(3)–C(11)	1.472(10)	1.469(2)
N(3)–C(14)	1.471(10)	1.461(2)
N(4)–C(12)	1.490(9)	1.473(2)
N(4)–C(15)	1.492(10)	1.492(2)
N(4)–C(13)	1.497(10)	1.471(2)
N(2)–C(3)	1.349(10)	1.333(2)
N(2)–C(2)	1.337(10)	1.349(2)
N(1)–C(2)	1.341(11)	1.321(3)
C(1)–N(1)	1.354(10)	1.343(2)
C(1)–S(1)–C(6)	90.9(4)	90.99(8)
H(1)–O(1)–C(17)	109.3	109.5
C(1)–N(1)–C(2)	128.0(8)	115.32(13)
C(14)–N(3)–C(3)	115.99(11)	116.83(13)
C(14)–N(3)–C(11)	108.9(7)	109.31(13)
C(15)–N(4)–C(12)	112.2(6)	112.79(12)
C(13)–N(4)–C(12)	109.30(10)	109.31(12)
C(13)–N(4)–C(15)	109.5(6)	109.36(12)
C(2)–N(1)–C(1)	113.34(46)	113.24(16)
C(2)–N(2)–C(3)	116.24(15)	117.36(16)

Table 4 Anti-plasmodial activities of tested compounds against the CQ-resistant W2 strain of *P. falciparum*

Compound code	IC_{50} (μM) ± SD	Compound code	IC_{50} (μM) ± SD
F1	2.4190 ± 0.1499	**F9**	6.4075 ± 0.2397
F2	1.3390 ± 0.0071	**F10**	3.9645 ± 0.1082
F3	1.0385 ± 0.0120	**F11**	1.1320 ± 0.0552
F4	**0.7515 ± 0.0442**	**F12**	1.3440 ± 0.1103
F5	1.1815 ± 0.0714	**F13**	1.2180 ± 0.1018
F6	1.0605 ± 0.2355	**F14**	1.1710 ± 0.0396
F7	1.6155 ± 0.0290	**F15**	2.2575 ± 0.1874
F8	1.3680 ± 0.1966	**F16**	**0.7488 ± 0.0196**
Chloroquine	0.1745 ± 0.0510		

respective compounds having R_3 = OCH_3 (**F9–F16**) except for compound **F16** (Table 4). Therefore, introduction of methoxy group on phenolic ring did not improve the antiplasmodial efficacy of the tested compounds. Furthermore, deep analysis into each group of compounds revealed that those having electron withdrawing substituent on the benzene ring are more active than those having electron releasing group. This might be due to the fact that electron withdrawing groups have compact electron cloud density while electron releasing groups have a more diffused electron cloud density which is sterically disturbing the bonding of compounds to the residue of targeted protein of *P. falciparum*. As evident, compound **F4** showed promising activity with IC_{50} 0.7515 μM against W2 strain of *P. falciparum* among all the compounds as well as its corresponding compounds. However, compound **F16**, also showed significant activity with IC_{50} 0.7488 μM against W2 strain of *P. falciparum*, opposite to the general activity trend of the series. This observation revealed that the combination of R_2 = CF_3 and R_3 = OCH_3 may results in such a favourable orientation of the molecule which may increase the interaction of the compound with the residue of active site of the target protein and lead to induce inhibition. Hence **F4** and **F16** are the best compounds which showed promising anti-plasmodial activity and further studies can be done to explore the insight.

2.4. Cytotoxicity assay

The compounds (**F3–F6** & **F16**) were evaluated for cytotoxicity against two cancer cells lines, human A549 (lung) and HeLa (cervical) cells in order to determine whether the mentioned activities are due to their anti-plasmodial efficacy or cytotoxicity (Table 5). As evident, the synthesized compounds displayed IC_{50} values in the range of 6.4–12.7 μM while doxorubicin exhibited an IC_{50} of 5.5 μM suggestive of the fact that these compounds can behave as good beginning for the synthesis of new pharmacological models against *P. falciparum*.

3. Physicochemical properties and ADME analysis

In silico physicochemical and pharmacokinetic properties of synthesized compounds is the most important method to develop a new drug candidate molecule. To determine the possible lead likeness of the best compounds (**F4**, **F3**, **F5**, **F6** and **F16**), physicochemical properties such as molecular weight (MW), hydrogen bond acceptors (HBA), number of hydrogen bond donors (HBD), number of rotatable bonds (RB), lipophilicity ($\log P$), topological polar surface area (TPSA) (Table 6) was predicted from the server Swiss ADME (http://www.swissadme.ch/). Furthermore, an online PreADMET method (http:/preadmet.bmdrc.org) was used to predict the pharmacokinetic profiles of these compounds (**F4**, **F3**, **F5**, **F6** and **F16**). The ADME predicted pharmacokinetic properties such as absorption of the human intestine (HIA percent), CaCo-2 skin permeability ($\log K_p$), MDCK (Madin–Darby canine kidney) cell permeability, plasma protein binding (%) and blood brain barrier penetration (Table 7). This investigation revealed that all compounds were predicted to display moderate permeability for Caco-2 cells. Compounds **F4**, **F3**, **F5**, **F6** and **F16** were assumed to display high human intestinal absorption. All the compounds were anticipated to show moderately strong plasma protein binding and very low MDCK permeability. All the synthesized compounds are expected to show low penetration into the central nervous system through blood–brain barrier. Test compounds were predicted not to inhibit CYP2C19 but inhibit CYP2C9, CYP2D6 and CYP3A4, indicating a high risk for interaction with drugs metabolized by the same enzymes. In addition, all the compounds were predicted to inhibit P-glycoprotein (P-gp) (Table 8).

4. Conclusion

In summary, this report presented the design, synthesis and validated by HRMS, ^{1}H NMR, ^{13}CNMR and furthermore, the

Table 5 Cytotoxicity of selected compounds against human A549 (lung) and HeLa (cervical) cancer cells and their selectivity index

Compounds	Cytotoxicity IC_{50} ± SD (μM)		*P. falciparum*[a] (CQ-R) W2 strain (μM)	Selectivity index[b] (SI)	Selectivity index[c] (SI)
	A549 (lung)	HeLa (cervical)			
F4	11.5 ± 0.4	10.3 ± 0.6	0.7515	15.302	13.70
F3	8.7 ± 0.6	12.7 ± 0.8	1.0320	8.43	12.30
F5	7.2 ± 0.3	9.1 ± 0.5	1.1815	6.09	7.70
F6	8.5 ± 0.4	6.4 ± 0.2	1.0605	8.01	6.03
F16	7.3 ± 0.3	7.1 ± 0.4	0.7488	9.86	9.59
Doxorubicin	5.5	5.7			

[a] CQ-R: chloroquine resistant strain. [b] SI: selective index is ratio of IC_{50} value of A549 (lung) cancer cell line to that of W2 resistant strain. [c] SI: selective index is ratio of IC_{50} value of HeLa (cervical) cancer cell line to that of W2 resistant strain.

Table 6 Physiochemical properties of target compounds (**F4**, **F3**, **F5**, **F6** and **F16**)

Compound	MW	Rot. bond	HBA	HBD	TPSA (Å^2)	clog *P*
F4	525.49	4	4	1	80.73	5.73
F3	492.58	4	6	1	80.73	5.29
F5	540.60	6	8	1	89.96	5.59
F6	509.04	4	5	1	80.73	5.50
F16	554.63	6	8	1	89.96	5.75
Required parameters[a]	≤500	≤10	≤10	≤5	≤140	2–5

[a] Calculated using Swiss ADME online server: MW = molecular weight; rot. bonds = number of rotatable bonds; HBD = number of hydrogen donors; HBA = number of hydrogen acceptors; TPSA = total polar surface area; clog *P* = log octanol/water partition coefficient.

Table 7 *In silico* ADME profiling of target compounds **F4**, **F3**, **F5**, **F6** and **F16** obtained from pre ADMET server

Sample code	Absorption			Distribution		
	Human intestinal absorption (HIA%)	Caco-2 cell permeability (nm s^{-1})	MDCK cell permeability (nm s^{-1})	Skin permeability (log K_p, cm h^{-1})	Plasma protein binding (%)	Blood–brain barrier penetration (C^{brain}/C^{blood})
F4	97.76	55.01	0.04	−3.04	91.26	0.39
F3	97.11	38.07	0.05	−3.59	87.48	0.11
F5	97.01	41.70	0.04	−1.92	82.28	0.45
F6	97.47	55.11	0.04	−3.42	84.61	0.20
F16	97.09	37.65	0.04	−2.27	84.49	0.13
Required parameters	>20	>4	>10	−6.1 to −0.19	>90	>0.1

Table 8 *In silico* metabolism profile of target compounds **F4**, **F3**, **F4**, **F5** and **F16** obtained from pre ADMET server

Sample code	CYP2C19 inhibition	CYP2C9 inhibition	CYP2D6 inhibition	CYP2D6 substrate	CYP3A4 inhibition	CYP3A4 substrate	Pgp inhibition
F4	None	Inhibitor	Inhibitor	Weakly	Inhibitor	Substrate	Inhibitor
F3	None	Inhibitor	Inhibitor	Substrate	Inhibitor	Substrate	Inhibitor
F5	None	Inhibitor	Inhibitor	Weakly	Inhibitor	Substrate	Inhibitor
F6	None	Inhibitor	Inhibitor	Weakly	Inhibitor	Substrate	Inhibitor
F16	None	Inhibitor	Inhibitor	Substrate	Inhibitor	Substrate	Inhibitor

structure integrity of the compound **F1** and **F2** were also confirmed by X-ray crystallography. The pharmacological evaluation of synthesised series of tetrahydrobenzothieno[2,3-*d*]pyrimidine derivatives with the purpose of studying their structure–activity relationship (SAR) against *P. falciparum*. Most of the synthesized molecules revealed significant *in vitro* antiplasmodial profiles with the activities being dependent upon the nature of substituent present on aromatic rings. Compounds **F4** which contain two chloro group on the benzene and absence of methoxy group on the phenolic ring showed best activity with IC_{50} 0.75 μM. **F16** also evidenced exceptionally best promising results opposite to general trend of the series, with IC_{50} 0.74 μM, respectively, against cultured *P. falciparum*. In addition, compounds (**F3–F6** and **F16**) were also screened for *in vitro* cytotoxicity against two cancer cell lines, human lung (A549) and cervical

(HeLa) cells, which showed non-cytotoxicity with significant selectivity indices. The *in silico* physicochemical and pharmacokinetics properties of the compounds (**F3–F6** and **F16**) indicated that these compounds have low toxicity with good absorption, penetration, and permeability properties. These compounds were predicted to inhibit CYP2C9, CYP2D6 and CYP3A4 and none of the compound showed inhibition towards CYP2C19, which indicates a high risk for interaction with drugs metabolized by the same enzymes. These results suggest that compounds **F4** and **F16** could be further investigated as lead molecules against *P. falciparum* and serve as templates for future drug-development. The pharmacological efficacy of these lead molecules against *P. falciparum* can be improved by incorporating or removing some chemical group which will lower their log*P* value. These changes may further enhance the bioavailability of these compounds.

5. Material and methods

5.1. Chemistry

The chemicals, reagents and solvents required for the synthesis and characterization of compounds were purchased from Sigma Aldrich, Alfa-Aesar and Spectrochem Pvt. Ltd. (India). The solvents were dried using standard methods. The melting points were determined with a Tanco PLT-276 apparatus and are uncorrected. Thin-layer chromatography was performed on a film of Merck silica gel (60–120) that contained a fluorescent indicator F254 supported on an aluminium dusted sheet of 0.25 mm thickness. Spots on these were detected under short (254 nm) and long (365 nm) wavelengths. ^{1}H NMR spectra were observed on a Bruker Avance 400 MHz spectrophotometer using deuterated chloroform ($CDCl_3$). Chemical shifts were demonstrated in δ (ppm), and tetramethylsilane was selected as an internal standard; multiplicities of NMR signals were labelled as s (singlet), d (doublet), dd (double doublet), t (triplet), q (quartet), m (multiplet, for unresolved lines). ^{13}C NMR spectra were recorded on a Bruker 101 MHz spectrometer in deuterated chloroform ($CDCl_3$). Mass spectra were recorded on an Agilent 6538 ultra high definition accurate mass-Q-TOF (LC-HRMS) instrument. Column chromatography was conducted on silica gel (SRL No. 63025 mesh 200–400) to obtained pure compounds.

5.1.1. Procedure for the synthesis of ethyl 2-amino-4,5,6,7-tetrahydrobenzo[*b*]thiophene-3-carboxylate (1). To the stirred solution of cyclohexanone (5 g, 50.9 mmol), ethyl cyanoacetate (5.75 g, 50.9 mmol) and elemental sulphur (1.83 g, 50.9 mmol) in absolute ethanol (20 mL), morpholine (4.43 g, 50.9 mmol) was added drop wise and heated to reflux for 7–8 h. The reaction mixture was cooled at room temperature. Excess solvent was expelled under reduced pressure, and the residue was poured into ice cold water. Yellow precipitate was obtained, filtered, and washed with water to give a yellow solid. This yellow solid was further purified by crystallisation in methanol to get pale yellow crystal in 90–95% yield.

5.1.2. Procedure for the synthesis of 5,6,7,8-tetrahydrobenzo[4,5]thieno[2,3-d]pyrimidin-4(3*H*)-one (2). Ethyl 2-amino-4,5,6,7-tetrahydrobenzo[*b*]thiophene-3-carboxylate **1** was suspended in formamide (400 mL) and refluxed for 4 h at 180 °C. After cooling to room temperature overnight, the dark brown needles were formed. These crystals were filtered and washed with cold water then drying under vacuum overnight (80–85% yield).

5.1.3. Procedure for the synthesis of 4-chloro-5,6,7,8-tetrahydrobenzo[4,5]thieno[2,3-*d*]pyrimidine (3). Cooled the solution of 5,6,7,8-tetrahydrobenzo[4,5]thieno[2,3-*d*] pyrimidin-4(3*H*)-one **2** (10 g, 48.5 mmol) in 40 mL of phosphorous oxychloride to 15–20 °C. Then, triethylamine (32 mL) was added drop wise into the solution maintaining the temperature below 20 °C. When addition was completed, then reaction mass was refluxed to 80 °C for 3 h. The progress of the reaction was scrutinized by TLC. After completion of reaction, the reaction mass was quenched in ice cold water with continuous stirring and product were obtained as yellow solid. Crude product was further purified by column chromatography using ethylacetate/petroleum ether (95 : 05) as the mobile phase to obtain pure 4-chloro-5,6,7,8-tetrahydrobenzo[4,5]thieno[2,3-*d*]pyrimidine **3** in 70–80% yield.

5.1.4. Procedure for the synthesis of 4-(piperazin-1-yl)-5,6,7,8-tetrahydrobenzo[4,5]thieno[2,3-*d*]pyrimidine (4). In a round bottom flask 4-chloro-5,6,7,8-tetrahydrobenzo[4,5] thieno[2,3-*d*]pyrimidine **3** (5 g, 22.25 mmol) was added to the stirred solution of anhydrous piperazine (5.74 g, 66.43 mmol) in dry methanol. The reaction mixture was refluxed at 70–80 °C for 4–5 h. The progress of reaction was monitored through TLC. After completion of reaction, filtered the white mass formed in the reaction mixture and washed several times with methanol. The filtrate was concentrated under reduced pressure to get solid residue. This residue was partitioned between chloroform and water. The combined organic layer splashed with brine solution and dried over anhydrous sodium sulphate. The solvent was expelled under reduced pressure, and the residual mass was purified by column chromatography to obtain pure 4-(piperazin-1-yl)-5,6,7,8-tetrahydrobenzo[4,5]thieno[2,3-*d*]pyrimidine **4** in 70–80% yield.

5.1.5. General procedure for synthesis of 2-((substituted)(4-(5,6,7,8tetrahydrobenzo[4,5]thieno[2,3-*d*]pyrimidin-4-yl) piperazin-1-yl)methyl)-6-substitutedphenol (F1–F16). To the stirred solution of 4-(piperazin-1-yl)-5,6,7,8-tetrahydrobenzo[4,5]thieno[2,3-d]pyrimidine **4** (0.5 g, 18.22 mmol) in DMF, salicylaldehyde/*ortho* vanillin (0.22 g, 18.22 mmol) was added in a drop wise fashion at room temperature. After 5 minutes, substituted boronic acid (18.22 mmol) was added to stirred solution and refluxed the reaction mixture at 60–70 °C for 12 h. The progress of reaction was monitored through TLC. After accomplishment of reaction, reaction mixture was poured drop wise with continuous stirring in ice cold water, white precipitate was separated out. Filtered the crude solid product and wash

several times with water and dried. Crude products were further purified by column chromatography to get pure **F** (**1**–**16**) compounds in 80–81% yield.

*5.1.5.1. 2-((4-Methoxyphenyl)(4-(5,6,7,8-tetrahydrobenzo[4,5]thieno[2,3-d]pyrimidin-4-yl)piperazin-1-yl)methyl)phenol (**F1**).* White solid, yield 80.0%; m.p. 105–107 °C; ^{1}H NMR (400 MHz, $CDCl_3$) δ (ppm) 11.70 (s, 1H), 8.50 (s, 1H), 7.37 (d, J = 7.6 Hz, 2H), 7.14–7.09 (m, 1H), 6.93 (dd, J = 7.6, 1.2 Hz, 1H), 6.87–6.82 (m, 3H), 6.72 (td, J = 7.6, 1.2 Hz, 1H), 4.44 (s, 1H), 3.76 (s, 3H), 3.50 (s, 4H), 2.85 (t, J = 6.0 Hz, 4H), 2.62 (s, 2H), 1.90–1.88 (m, 2H), 1.78–1.76 (m, 4H); ^{13}C NMR (101 MHz, $CDCl_3$) δ 168.86, 162.17, 159.80, 156.57, 151.95, 135.84, 132.17, 130.13, 129.67, 129.02, 127.42, 125.86, 121.78, 120.03, 117.53, 114.73, 76.42, 60.86, 55.69, 50.95, 27.16, 26.26, 23.44, 23.27. HRMS m/z calcd for $C_{28}H_{30}N_4O_2S$ $[M + H]^+$ 487.2168 found 487.2164.

*5.1.5.2. 2-((4-(5,6,7,8-Tetrahydrobenzo[4,5]thieno[2,3-d]pyrimidin-4-yl)piperazin-1-yl)(p-tolyl)methyl)phenol (**F2**).* White solid, yield 80.5%; m.p. 107–108 °C; ^{1}H NMR (400 MHz, $CDCl_3$) δ (ppm) 11.69 (s, 1H), 8.51 (s, 1H), 7.35 (d, J = 6.8 Hz, 2H), 7.13–7.09 (m, 3H), 6.95 (d, J = 7.6 Hz, 1H), 6.88 (d, J = 8.0 Hz, 1H), 6.72 (t, J = 7.4 Hz, 1H), 4.45 (s, 1H), 3.51 (s, 4H), 2.86 (t, J = 6.0 Hz, 4H), 2.64 (s, 2H), 2.30 (s, 3H), 1.91–1.88 (m, 2H), 1.81–1.77 (m, 4H); ^{13}C NMR (101 MHz, $CDCl_3$) δ 168.87, 162.19, 156.57, 151.97, 137.16, 135.85, 130.14, 129.68, 129.05, 128.78, 127.42, 125.67, 121.73, 120.04, 117.52, 76.78, 51.92, 50.95, 27.17, 26.27, 23.44, 23.28. HRMS m/z calcd for $C_{28}H_{30}N_4OS$ $[M + H]^+$ 471.2219 found 471.2216.

*5.1.5.3. 2-((3,4-Difluorophenyl)(4-(5,6,7,8-tetrahydrobenzo[4,5]thieno[2,3-d]pyrimidin-4-yl)piperazin-1-yl)methyl)phenol (**F3**).* White solid, yield 80.0%; m.p. 200–202 °C; ^{1}H NMR (400 MHz, $CDCl_3$) δ (ppm) 11.39 (s, 1H), 8.52 (s, 1H), 7.39–7.30 (m, 1H), 7.17–7.07 (m, 3H), 6.91 (dd, J = 18.8, 7.2 Hz, 2H), 6.76 (t, J = 7.2 Hz, 1H), 4.42 (s, 1H), 3.53 (s, 4H), 2.86 (t, J = 5.2 Hz, 4H), 2.62 (s, 2H), 1.90–1.89 (m, 2H), 1.80–1.78 (m, 2H), 1.72 (s, 2H); ^{13}C NMR (101 MHz, $CDCl_3$) δ 168.94, 162.00, 156.20, 151.94, 137.29, 135.90, 129.46, 127.23, 124.75, 121.84, 120.32, 117.90, 76.13, 51.93, 50.84, 27.14, 26.26, 23.42, 23.26. HRMS m/z calcd for $C_{27}H_{26}F_2N_4OS$ $[M + H]^+$ 493.1899 found 493.1870.

*5.1.5.4. 2-((3,4-Dichlorophenyl)(4-(5,6,7,8-tetrahydrobenzo[4,5]thieno[2,3-d]pyrimidin-4-yl)piperazin-1-yl)methyl)phenol (**F4**).* White solid, yield 81.0%; m.p. 225–227 °C; ^{1}H NMR (400 MHz, $CDCl_3$) δ (ppm) 11.33 (s, 1H), 8.52 (s, 1H), 7.55 (s, 1H), 7.40–7.34 (m, 2H), 7.17–7.14 (m, 1H), 6.94–6.88 (m, 2H), 6.76 (t, J = 7.2 Hz, 1H), 4.41 (s, 1H), 3.52 (s, 4H), 2.87 (s, 4H), 2.63 (s, 2H), 1.91–1.89 (m, 2H), 1.80–1.79 (m, 2H), 1.62 (s, 2H); ^{13}C NMR (101 MHz, $CDCl_3$) δ 168.47, 162.06, 156.28, 151.96, 140.48, 136.07, 131.60, 130.73, 129.66, 129.52, 127.29, 124.54, 121.85, 120.36, 117.94, 76.00, 60.59, 52.00, 50.83, 27.13, 26.26, 23.42, 23.26. HRMS m/z calcd for $C_{27}H_{26}Cl_2N_4OS$ $[M + H]^+$ 525.1283 found 525.1278.

*5.1.5.5. 2-((4-(5,6,7,8-Tetrahydrobenzo[4,5]thieno[2,3-d]pyrimidin-4-yl)piperazin-1-yl)(4-(trifluoromethoxy)phenyl)methyl)phenol (**F5**).* White solid, yield 80.5%; m.p. 210–211 °C; ^{1}H NMR (400 MHz, $CDCl_3$) δ (ppm) 11.49 (s, 1H), 8.51 (s, 1H), 7.46 (s, 2H), 7.17–7.13 (m, 3H), 6.95–6.88 (m, 2H), 6.77–6.73 (t, J = 7.2 Hz, 1H), 4.48 (s, 1H), 3.52 (s, 4H), 2.86 (s, 4H), 2.61 (s, 2H), 1.88–1.78 (m, 6H); ^{13}C NMR (101 MHz, $CDCl_3$) δ 168.91, 162.09, 156.36, 151.94, 149.36, 138.97, 136.00, 130.26, 129.62, 129.46, 127.34, 125.13, 121.84, 120.26, 119.56, 117.80, 76.31, 51.91, 50.87, 27.13, 26.26, 23.42, 23.26. HRMS m/z calcd for $C_{28}H_{27}F_3N_4O_2S$ $[M + H]^+$ 541.1885 found 541.0176.

*5.1.5.6. 2-((3-Chloro-4-fluorophenyl)(4-(5,6,7,8-tetrahydrobenzo[4,5]thieno[2,3-d]pyrimidin-4-yl)piperazin-1-yl)methyl)phenol (**F6**).* White solid, yield 80.5%; m.p. 217–218 °C; ^{1}H NMR (400 MHz, $CDCl_3$) δ (ppm) 11.39 (s, 1H), 8.51 (s, 1H), 7.51 (d, J = 4.4 Hz, 1H), 7.38 (s, 1H), 7.12 (dt, J = 17.1, 8.0 Hz, 2H), 6.91 (m, 2H), 6.76 (m, 1H), 4.41 (s, 1H), 3.52 (s, 4H), 2.86 (s, 4H), 2.61 (s, 2H), 1.91 (s, 2H), 1.80–1.71 (m, 4H). ^{13}C NMR (101 MHz, $CDCl_3$) δ 168.88, 162.00, 159.47, 156.99, 156.28, 151.94, 137.39, 135.98, 130.97, 129.55, 128.49, 127.31, 124.80, 121.84, 120.33, 117.92, 117.82, 117.57, 76.01, 52.01, 50.84, 27.14, 26.27, 23.42, 23.26. HRMS m/z calcd for $C_{27}H_{26}ClFN_4OS$ $[M + H]^+$ 509.1578 found 509.1583.

*5.1.5.7. 2-((4-Fluorophenyl)(4-(5,6,7,8-tetrahydrobenzo[4,5]thieno[2,3-d]pyrimidin-4-yl)piperazin-1-yl)methyl)phenol (**F7**).* White solid, yield 80.5%; m.p. 160–165 °C; ^{1}H NMR (400 MHz, $CDCl_3$) δ (ppm) 11.60 (s, 1H), 8.53 (s, 1H), 7.52–7.40(m, 2H), 7.18–7.14 (m, 2H), 7.02 (t, J = 7.6 Hz, 1H), 6.96 (d, J = 7.6 Hz, 1H), 6.91 (d, J = 8.4 Hz, 1H), 6.76 (t, J = 6.0 Hz, 1H), 4.49 (s, 1H), 3.54 (s, 4H), 2.88 (t, J = 5.6 Hz, 4H), 2.72–2.55 (m, 2H), 1.93–1.91 (m, 2H), 1.82–1.79 (m, 4H); ^{13}C NMR (101 MHz, $CDCl_3$) δ 168.90, 164.05, 162.12, 161.66, 156.43, 151.95, 136.07, 135.96, 130.54, 129.63, 129.31, 127.37, 125.42, 121.82, 120.18, 117.72, 116.49, 116.28, 76.12, 51.89, 50.90, 27.15, 26.26, 23.43, 23.27.HRMS m/z calcd for $C_{27}H_{27}FN_4OS$ $[M + H]^+$ 475.1968 found 475.1973.

*5.1.5.8. 2-((4-(5,6,7,8-Tetrahydrobenzo[4,5]thieno[2,3-d]pyrimidin-4-yl)piperazin-1-yl)(4-(trifluoromethyl)phenyl)methyl)phenol (**F8**).* White solid, yield 81.0%; m.p. 161–162 °C; ^{1}H NMR (400 MHz, $CDCl_3$) δ (ppm) 11.26 (s, 1H), 8.51 (s, 1H), 7.60–7.56 (m, H), 7.14 (t, J = 8.0 Hz, 1H), 6.96 (d, J = 8.0 Hz, 1H), 6.89 (d, J = 8.04 Hz, 1H), 6.74 (t, J = 7.6 Hz, 1H), 4.52 (s, 1H), 3.52 (s, 4H), 2.86 (t, J = 5.6 Hz, 4H), 2.77–2.55 (m, 2H), 1.89–1.82 (m, 2H), 1.79–1.78 (m, 4H). ^{13}C NMR (101 MHz, $CDCl_3$) δ 168.95, 162.09, 156.33, 151.93, 144.73, 136.07, 129.60, 129.57, 127.30, 126., 124.77, 123.00, 121.85, 120.34, 117.86, 76.71, 60.87, 52.00, 50.85, 27.13, 26.25, 23.41, 23.25. HRMS m/z calcd for $C_{28}H_{27}F_3N_4OS$ $[M + H]^+$ 525.1936 found 525.1935.

*5.1.5.9. 2-Methoxy-6-((4-methoxyphenyl)(4-(5,6,7,8-tetrahydrobenzo[4,5]thieno[2,3-d]pyrimidin-4-yl)piperazin-1-yl)methyl)phenol (**F9**).* White solid, yield 80.0%; m.p. 145–147 °C; H NMR (500 MHz, $CDCl_3$) δ 11.86 (s, 1H), 8.50 (s, 1H), 7.37 (d, J = 10.0 Hz, 2H), 6.83 (d, J = 8.5 Hz, 2H), 6.75 (d, J = 1 Hz, 1H), 6.70 (t, J = 7.5 Hz, 1H), 6.58 (d, J = 7.5 Hz, 1H), 4.45 (s, 1H), 3.89 (s, 3H), 3.77 (s, 3H), 2.89–2.82 (m, 8H), 2.66–2.58 (m, 2H), 1.90–1.88 (m, 2H), 1.80–1.77 (m, 4H). ^{13}C NMR (126 MHz, $CDCl_3$) δ 169.64, 163.89, 161.87, 159.09, 158.93, 151.55, 148.38, 145.53, 135.09, 131.82, 126.10, 121.12, 119.09, 114.42, 110.74, 75.33, 56.21, 54.92, 50.56, 27.13, 25.79, 22.76.HRMS m/z calcd for $C_{29}H_{32}N_4O_3S$ $[M + H]^+$ 517.2273 found 517.2271.

*5.1.5.10. 2-Methoxy-6-((4-(5,6,7,8-tetrahydrobenzo[4,5]thieno[2,3-d]pyrimidin-4-yl)piperazin-1-yl)(p-tolyl)methyl)phenol (**F10**).* White

solid, yield 80.0%; m.p.168–169 °C; ^{1}H NMR (500 MHz, $CDCl_3$) δ 11.81 (s, 1H), 8.50 (s, 1H), 7.35 (d, J = 8.8 Hz, 2H), 7.11 (d, J = 8.0 Hz, 2H), 6.74 (d, J = 1.5 Hz, 1H), 6.69 (t, J = 7.5 Hz, 1H), 6.59 (d, J = 7.5 Hz, 1H), 4.45 (s, 1H), 3.89 (s, 3H), 2.90–2.82 (m, 8H), 2.69–2.57 (m, 2H), 2.30 (s, 3H), 1.91–1.88 (m, 2H), 1.80–1.77 (m, 4H).^{13}C NMR (126 MHz, $CDCl_3$) δ 168.58, 161.27, 151.85, 148.53, 145.15, 137.47, 136.19, 135.51, 129.80, 128.12, 127.16, 125.50, 121.42, 119.48, 110.05, 75.94, 55.90, 50.55, 27.12, 25.47, 23.14, 21.47. HRMS m/z calcd for $C_{29}H_{32}N_4O_2S$ $[M + H]^+$ 501.2324 found 501.2321.

5.1.5.11. 2-((3,4-Difluorophenyl)(4-(5,6,7,8-tetrahydrobenzo[4,5]thieno[2,3-d]pyrimidin-4-yl)piperazin-1-yl)methyl)-6-methoxyphenol ***(F11)****.* White solid, yield 81.0%; m.p. 185–187 °C; ^{1}H NMR (400 MHz, $CDCl_3$) δ (ppm) 11.10 (s, 1H), 8.52 (s, 1H), 7.36 (s, 1H), 7.15–7.07 (m, 2H), 6.81–6.72 (m, 3H), 4.48 (s, 1H), 3.91 (s, 3H), 2.90–2.87 (m, 8H), 2.63 (s, 2H), 1.93–1.89 (m, 2H), 1.83–1.79 (m, 4H); ^{13}C NMR (101 MHz, $CDCl_3$) δ 169.01, 162.08, 152.00, 149.71, 148.79, 145.44, 137.34, 135.91, 127.43, 125.66, 124.89, 121.70, 121.13, 120.14, 118.14, 117.62, 111.22, 75.00, 56.39, 51.90, 50.81, 31.36, 27.16, 26.25, 23.41, 23.26. HRMS m/z calcd for $C_{28}H_{28}F_2N_4O_2S$ $[M + H]^+$ 523.1979 found 523.1975.

5.1.5.12. 2-((3,4-Dichlorophenyl)(4-(5,6,7,8-tetrahydrobenzo[4,5]thieno[2,3-d]pyrimidin-4-yl)piperazin-1-yl)methyl)-6-methoxyphenol ***(F12)****.* White solid, yield 80.5%; m.p. 222–224 °C; ^{1}H NMR (400 MHz, $CDCl_3$) δ (ppm) ^{1}H NMR (400 MHz, $CDCl_3$) δ 10.91 (s, 1H), 8.53 (s, 1H), 7.57 (s, 1H), 7.40 (s, 2H), 6.84–6.74 (m, 2H), 6.66 (s, 1H), 4.48 (s, 1H), 3.90 (s, 3H), 2.88–2.87 (m, 8H), 2.64 (s, 2H), 1.93–1.89 (m, 2H), 1.83–1.79 (m, 4H); ^{13}C NMR (101 MHz, $CDCl_3$) δ 168.91, 162.01, 151.92, 148.75, 145.44, 140.82, 135.92, 133.26, 132.59, 131.53, 130.69, 127.95, 127.35, 125.12, 125.00, 121.72, 121.10, 120.19, 111.25, 74.71, 56.39, 51.96, 50.83, 27.17, 26.25, 23.42, 23.27. HRMS m/z calcd for $C_{28}H_{28}Cl_2N_4O_2S$ $[M + H]^+$ 556.5259 found 556.5251.

5.1.5.13. 2-Methoxy-6-((4-(5,6,7,8-tetrahydrobenzo[4,5]thieno[2,3-d]pyrimidin-4-yl)piperazin-1-yl)(4-(trifluoromethoxy)phenyl)methyl) phenol ***(F13)****.* White solid, yield 81.0%; m.p. 175–177 °C;^{1}H NMR (400 MHz, $CDCl_3$) δ (ppm) 11.34 (s, 1H), 8.53 (s, 1H), 7.53 (d, J = 8.0 Hz, 2H), 7.17 (d, J = 8.0 Hz, 2H), 6.81–6.73 (m, 3H), 4.53 (s, 1H), 3.91 (s, 3H), 2.88 (t, J = 4.0 Hz, 8H), 2.0.69–2.56 (t, J = 24 Hz, 2H), 1.93–1.91 (t, J = 4.0 Hz, 2H), 1.83–1.78 (m, 4H). ^{13}C NMR (101 MHz, $CDCl_3$) δ 168.73, 161.97, 151.84, 149.34, 148.82, 145.58, 139.05, 135.91, 130.24, 127.36, 125.58, 122.12, 121.79, 121.68, 121.26, 120.39, 120.04, 119.56, 111.15, 75.46, 51.96, 50.83, 27.18, 23.41, 23.26. HRMS m/z calcd for $C_{29}H_{29}F_3N_4O_3S$ $[M + H]^+$ 571.1991 found 571.1981.

5.1.5.14. 2-((3-Chloro-4-fluorophenyl)(4-(5,6,7,8-tetrahydrobenzo[4,5]thieno[2,3-d]pyrimidin-4-yl)piperazin-1-yl)methyl)-6-methoxyphenol ***(F14)****.* White solid, yield 80.5%; m.p. 216–215 °C; ^{1}H NMR (400 MHz, $CDCl_3$) δ (ppm) 11.14 (s, 1H), 8.53 (s, 1H), 7.64–7.57 (m, 3H), 6.81–6.74 (m, 3H), 4.58 (s, 1H), 3.91 (s, 3H), 2.88 (t, J = 4.0 Hz, 8H), 2.65 (t, J = 16.0 Hz, 2H), 1.92 (t, J = 4.0 Hz, 2H), 1.83–1.79 (m, 4H).

^{13}C NMR (101 MHz, CDCl3) δ 168.94, 161.98, 151.92, 148.75, 145.53, 144.57, 135.90, 129.08, 127.33, 126.46, 125.75, 125.30, 121.71, 121.18, 120.13, 111.24, 75.59, 56.39, 52.02, 50.84, 31.34, 27.16, 26.25, 23.41, 23.27. HRMS m/z calcd for $C_{28}H_{28}ClFN_4O_2S$ $[M + H]^+$ 540.0713 found 540.0712.

5.1.5.15. 2-((4-Fluorophenyl)(4-(5,6,7,8-tetrahydrobenzo[4,5]thieno[2,3-d]pyrimidin-4-yl)piperazin-1-yl)methyl)-6-methoxyphenol (F15). White solid, yield 80.5%; m.p. 202–203 °C; ^{1}H NMR (400 MHz, $CDCl_3$) δ (ppm) 11.56 (s, 1H), 8.52 (s, 1H), 7.46 (s, 1H), 7.03–6.99 (m, 4H), 6.77 (d, J = 4.0 Hz, 1H), 6.74 (t, J = 8.0 Hz, 1H), 6.61 (d, J = 4.0 Hz, 2H), 4.50 (s, 1H), 3.91 (s, 3H), 2.88 (t, J = 4.0 Hz, 8H), 2.63 (s, 2H), 1.93–1.91 (m, 2H), 1.83–1.79 (m, 4H). ^{13}C NMR (101 MHz, $CDCl_3$) δ 168.83, 164.12, 162.01, 161.67, 151.93, 148.84, 145.68, 136.10, 135.82, 130.57, 130.50, 127.38, 125.84, 121.68, 121.31, 119.92, 116.44, 116.23, 111.06, 75.66, 56.36, 51.95, 50.86, 27.18, 26.25, 23.42, 23.27. HRMS m/z calcd for $C_{28}H_{29}FN_4O_2S$ $[M + H]^+$ 505.2074 found 505.2070.

5.1.5.16. 2-Methoxy-6-((4-(5,6,7,8-tetrahydrobenzo[4,5]thieno[2,3-d]pyrimidin-4-yl)piperazin-1-yl)(4-(trifluoromethyl) phenyl)methyl)phenol ***(F16)****.* White solid, yield 81.0%; m.p. 150–152 °C; ^{1}H NMR (400 MHz, $CDCl_3$) δ (ppm) 11.05 (s, 1H), 8.52 (s, 1H), 7.53 (d, J = 8.0 Hz, 2H), 7.40 (s, 2H), 7.09 (t, J = 8.0 Hz, 1H), 6.79 (d, J = 4.0 Hz, 1H), 6.76 (d, J = 8.0 Hz, 1H), 4.48 (s, 1H), 3.90 (s, 3H), 2.87 (t, J = 8.0 Hz, 8H), 2.63 (s, 2H), 1.91 (t, J = 4.0 2H), 1.83–1.77 (m, 4H). ^{13}C NMR (101 MHz, $CDCl_3$) δ 168.90, 161.99, 159.39, 156.91, 151.92, 148.78, 145.46, 137.66, 135.88, 130.92, 128.51, 128.44, 127.35, 125.32, 121.86, 121.70, 121.13, 120.12, 117.69, 117.48, 111.19, 74.80, 56.37, 51.93, 50.82, 31.34, 27.16, 26.24, 23.41, 23.26. HRMS m/z calcd for $C_{29}H_{29}F_3N_4O_2S$ $[M + H]^+$ 555.2042 found 555.2045.

5.2. Procedure for X-ray crystallographic study

The crystal structure of prepared compounds **F1** and **F2** were obtained *via* single-crystal X-ray diffraction. The slow evaporation of ethyl acetate solutions of compounds **F1** and **F2** gave colourless crystals that were boarded upon loops having mineral oil. An automated Bruker SMART APEX CCD diffractometer provided with fine focus sealed tube (1.75 kW) Mo Kα X-ray source (λ = 0.71073 Å) with uplifting ω (width of 0.3° per frame) at 5 frame s^{-1} visualising speed was used to acquire the geometric and intensity data using the ω–2θ scan mode and then amended for Lorentz-polarization and absorption effects.[46] WinGx (version 1.63.04a) was used to solve as well as enhance the structures through the SHELXL-2013 method.[47] All non-hydrogen atoms were polished with anisotropic displacement coefficients and non-hydrogen atom coordinates were approved to be on their subsequent carbon atoms. The final improvement included atomic sites for all atoms, isotropic thermal factors for hydrogen atoms, and anisotropic thermal factors for non-hydrogen atoms. The structural views of compounds **F1** and **F2** were acquired with ORTEP.[48] Further details are given in Table 3. The CCDC deposition number for **F1** is 2 008 067 and **F2** is 2 008 065.

5.3. Assessment of the antiplasmodial activity of synthesised compounds

W2 strain of *P. falciparum* was cultured and compound sensitivities were determined as previously described.[49] In

brief, microwell cultures were incubated with various concentrations of the prepared compounds, added from DMSO stocks, for 48 h beginning at the ring stage. After 48 h, when control cultures contained nearly all new ring-stage parasites, parasites were fixed with 1% formaldehyde in PBS, pH 7.4, for 48 h at RT and labeled with YOYO-1 (1 nM; Molecular Probes) in 0.1% Triton X-100 in PBS. Parasitemias were evaluated from dot plots (forward scatter *vs.* fluorescence) developed on a FACSort flow cytometer using CELLQUEST software (Becton Dickinson). IC_{50} values for growth inhibition were evaluated with GraphPad Prism software from plots of percentage parasitemia compared to controls (untreated parasites) over inhibitor concentration. In each case, the goodness of curve fit was documented by R^2 values of >0.95.

5.4. Cytotoxicity assay

The cytotoxicity of best compounds (**F3–F6** and **F16**) and doxorubicin was determined using A549 (lung) and HeLa (cervical) cancer cells grown in Dulbecco's modified Eagle's medium (DMEM, Gibco, USA) augmented with 10% fetal bovine serum. Cells were seeded in 96-well plates in 160 μL medium at a density of 1×10^4 cells per well and incubated for 24 h to allow cells to adhere at 37 °C. Furthermore, the complexes were added with different concentrations into all the cultured plates except 3 cell wells, studied as control wells. After 24 h compound incubation, the media were removed from wells including control wells. Subsequently, 25 μL of 4 mg mL^{-1} of MTT was added to each well and incubated for an additional 4 h. At the later stage, an amount of 200 μL of DMSO was used to dissolve the formazan crystals after discarding the media. The IC_{50} values were plotted in GraphPad Prism, version 7, using nonlinear regression analysis method. The percentage survival was determined by comparison with control wells. Values obtained from three independent experiments were used to calculate IC_{50} values with the log (inhibitor) *vs.* response nonlinear regression function of the GraphPad Prism software.

6. Physicochemical properties and ADME analysis

The physicochemical and pharmacokinetic profiles of best compounds (**F3**, **F4**, **F5**, **F6** and **F16**) were predicted using online server SwissADME (http://www.swissadme.ch/)[50] and PreADMET (http://preadmet.bmdrc.org).[51] The prediction of physicochemical properties of best compounds like molecular weight (MW), hydrogen bond acceptors (HBA), number of hydrogen bond donors (HBD), number of rotatable bonds (RB), lipophilicity ($\log P$), topological polar surface area (TPSA) was done by SwissADME online tool. *In silico* ADME analysis determines pharmacokinetic properties like human intestinal absorption (HIA%), colon adenocarcinoma (Caco-2) cell permeability, skin permeability, plasma protein binding, blood brain barrier (BBB), Madin–Darby canine kidney (MDCK) cell permeability, blood–brain barrier (BBB) penetration.

Abbreviations used

P. falciparum	*Plasmodium falciparum*
SAR	Structure activity relationship
NMR	Nuclear Magnetic Resonance
ADMET	Absorption, distribution, metabolism, excretion, and toxicity
CQ	Chloroquine
ACT	Artemisinin based combination therapy
PfDHFR	*Plasmodium falciparum* dihydrofolate reductase
$POCl_3$	Phosphorous oxychloride
MDCK	Madin–Darby canine kidney
rt	Room temperature
m.p.	Melting point
UV	Ultraviolet
TLC	Thin layer chromatography
ppm	Parts per million
DMSO	Dimethyl sulfoxide
DMEM	Dulbecco's modified Eagle's medium

Conflicts of interest

There are no conflicts of interest to declare.

Acknowledgements

Kavita Pal is thankful to University Grants Commission, Government of India, for financial assistance through Central University Ph.D. Students Fellowship.

References

1 E. A. Ashley, A. Pyae Phyo and C. J. Woodrow, *Lancet*, 2018, **391**, 1608–1621.
2 C. J. Murray, L. C. Rosenfeld, S. S. Lim, K. G. Andrews, K. J. Foreman, D. Haring, N. Fullman, M. Naghavi, R. Lozano and A. D. Lopez, *Lancet*, 2012, **379**, 413–431.
3 WHO, *World malaria report 2020: 20 years of global progress and challenges*, 2020.
4 T. G. Geary and P. J. Rosenthal, *J. Parasitol.*, 2002, **88**, 520.
5 P. F. Salas, C. Herrmann and C. Orvig, *Chem. Rev.*, 2013, **113**, 3450–3492.
6 M. Mushtaque and Shahjahan, *Eur. J. Med. Chem.*, 2015, **90**, 280–295.
7 S. Singh, D. Agarwal, K. Sharma, M. Sharma, M. A. Nielsen, M. Alifrangis, A. K. Singh, R. D. Gupta and S. K. Awasthi, *Eur. J. Med. Chem.*, 2016, **122**, 394–407.
8 M. Sinha, V. R. Dola, A. Soni, P. Agarwal, K. Srivastava, W. Haq, S. K. Puri and S. B. Katti, *Bioorg. Med. Chem.*, 2014, **22**, 5950–5960.
9 R. M. Beteck, F. J. Smit, R. K. Haynes and D. D. N'Da, *Malar. J.*, 2014, **13**, 339.

10 A. M. Dondorp, S. Yeung, L. White, C. Nguon, N. P. J. Day, D. Socheat and L. von Seidlein, *Nat. Rev. Microbiol.*, 2010, **8**, 272–280.
11 K. M. Tun, M. Imwong, K. M. Lwin, A. A. Win, T. M. Hlaing, T. Hlaing, K. Lin, M. P. Kyaw, K. Plewes, M. A. Faiz, M. Dhorda, P. Y. Cheah, S. Pukrittayakamee, E. A. Ashley, T. J. C. Anderson, S. Nair, M. McDew-White, J. A. Flegg, E. P. M. Grist, P. Guerin, R. J. Maude, F. Smithuis, A. M. Dondorp, N. P. J. Day, F. Nosten, N. J. White and C. J. Woodrow, *Lancet Infect. Dis.*, 2015, **15**, 415–421.
12 A. P. Phyo, S. Nkhoma, K. Stepniewska, E. A. Ashley, S. Nair, R. McGready, C. ler Moo, S. Al-Saai, A. M. Dondorp, K. M. Lwin, P. Singhasivanon, N. P. Day, N. J. White, T. J. Anderson and F. Nosten, *Lancet*, 2012, **379**, 1960–1966.
13 S. Takala-Harrison, C. G. Jacob, C. Arze, M. P. Cummings, J. C. Silva, A. M. Dondorp, M. M. Fukuda, T. T. Hien, M. Mayxay, H. Noedl, F. Nosten, M. P. Kyaw, N. T. T. Nhien, M. Imwong, D. Bethell, Y. Se, C. Lon, S. D. Tyner, D. L. Saunders, F. Ariey, O. Mercereau-Puijalon, D. Menard, P. N. Newton, M. Khanthavong, B. Hongvanthong, P. Starzengruber, H.-P. Fuehrer, P. Swoboda, W. A. Khan, A. P. Phyo, M. M. Nyunt, M. H. Nyunt, T. S. Brown, M. Adams, C. S. Pepin, J. Bailey, J. C. Tan, M. T. Ferdig, T. G. Clark, O. Miotto, B. MacInnis, D. P. Kwiatkowski, N. J. White, P. Ringwald and C. V. Plowe, *J. Infect. Dis.*, 2015, **211**, 670–679.
14 F. W. Muregi and A. Ishih, *Drug Dev. Res.*, 2010, **71**, 20–32.
15 F. Simon, *Nat. Rev. Drug Discovery*, 2006, **5**, 881–882.
16 J. Walsh and A. Bell, *Curr. Pharm. Des.*, 2009, **15**, 2970–2985.
17 S. Vangapandu, S. Sachdeva, M. Jain, S. Singh, P. P. Singh, C. L. Kaul and R. Jain, *Bioorg. Med. Chem.*, 2003, **11**, 4557–4568.
18 A. Çapcı, M. M. Lorion, H. Wang, N. Simon, M. Leidenberger, M. C. Borges Silva, D. R. M. Moreira, Y. Zhu, Y. Meng, J. Y. Chen, Y. M. Lee, O. Friedrich, B. Kappes, J. Wang, L. Ackermann and S. B. Tsogoeva, *Angew. Chem., Int. Ed.*, 2019, **58**, 13066–13079.
19 M. Bassetto, P. Leyssen, J. Neyts, M. M. Yerukhimovich, D. N. Frick and A. Brancale, *Eur. J. Med. Chem.*, 2016, **123**, 31–47.
20 O. H. Rizk, O. G. Shaaban and I. M. El-Ashmawy, *Eur. J. Med. Chem.*, 2012, **55**, 85–93.
21 K. Bozorov, J.-Y. Zhao, B. Elmuradov, A. Pataer and H. A. Aisa, *Eur. J. Med. Chem.*, 2015, **102**, 552–573.
22 B. Wilding and N. Klempier, *Org. Prep. Proced. Int.*, 2017, **49**, 183–215.
23 Y. Kotaiah, N. Harikrishna, K. Nagaraju and C. Venkata Rao, *Eur. J. Med. Chem.*, 2012, **58**, 340–345.
24 W. A. El-Sayed, O. M. Ali, R. A. F. Zyada, A. A. Mohamed and A. A. H. Abdel-Rahman, *Acta Pol. Pharm.*, 2012, **69**, 439–447.
25 S.-G. Li, C. Vilchèze, S. Chakraborty, X. Wang, H. Kim, M. Anisetti, S. Ekins, K. Y. Rhee, W. R. Jacobs and J. S. Freundlich, *Tetrahedron Lett.*, 2015, **56**, 3246–3250.
26 S. Leeza Zaidi, S. M. Agarwal, P. Chavalitshewinkoon-Petmitr, T. Suksangpleng, K. Ahmad, F. Avecilla and A. Azam, *RSC Adv.*, 2016, **6**, 90371–90383.
27 J. L. Woodring, G. Patel, J. Erath, R. Behera, P. J. Lee, S. E. Leed, A. Rodriguez, R. J. Sciotti, K. Mensa-Wilmot and M. P. Pollastri, *MedChemComm*, 2015, **6**, 339–346.
28 A. Rosowsky, K. K. N. Chen and M. Lin, *J. Med. Chem.*, 1973, **16**, 191–194.
29 M. Chaykovsky, M. Lin, A. Rosowsky and E. J. Modest, *J. Med. Chem.*, 1973, **16**, 188–191.
30 J. C. Aponte, A. J. Vaisberg, D. Castillo, G. Gonzalez, Y. Estevez, J. Arevalo, M. Quiliano, M. Zimic, M. Verástegui, E. Málaga, R. H. Gilman, J. M. Bustamante, R. L. Tarleton, Y. Wang, S. G. Franzblau, G. F. Pauli, M. Sauvain and G. B. Hammond, *Bioorg. Med. Chem.*, 2010, **18**, 2880–2886.
31 J. L. Woodring, R. Behera, A. Sharma, J. Wiedeman, G. Patel, B. Singh, P. Guyett, E. Amata, J. Erath, N. Roncal, E. Penn, S. E. Leed, A. Rodriguez, R. J. Sciotti, K. Mensa-Wilmot and M. P. Pollastri, *ACS Med. Chem. Lett.*, 2018, **9**, 996–1001.
32 D. González Cabrera, C. Le Manach, F. Douelle, Y. Younis, T.-S. Feng, T. Paquet, A. T. Nchinda, L. J. Street, D. Taylor, C. de Kock, L. Wiesner, S. Duffy, K. L. White, K. M. Zabiulla, Y. Sambandan, S. Bashyam, D. Waterson, M. J. Witty, S. A. Charman, V. M. Avery, S. Wittlin and K. Chibale, *J. Med. Chem.*, 2014, **57**, 1014–1022.
33 C. D. Edlin, G. Morgans, S. Winks, S. Duffy, V. M. Avery, S. Wittlin, D. Waterson, J. Burrows and J. Bryans, *ACS Med. Chem. Lett.*, 2012, **3**, 570–573.
34 I. Donkor, *Eur. J. Med. Chem.*, 2003, **38**, 605–611.
35 A. Gangjee, W. Li, R. L. Kisliuk, V. Cody, J. Pace, J. Piraino and J. Makin, *J. Med. Chem.*, 2009, **52**, 4892–4902.
36 A. Gangjee, Y. Qiu, W. Li and R. L. Kisliuk, *J. Med. Chem.*, 2008, **51**, 5789–5797.
37 B. Tarnchompoo, P. Chitnumsub, A. Jaruwat, P. J. Shaw, J. Vanichtananukul, S. Poen, R. Rattanajak, C. Wongsombat, A. Tonsomboon, S. Decharuangsilp, T. Anukunwithaya, U. Arwon, S. Kamchonwongpaisan and Y. Yuthavong, *ACS Med. Chem. Lett.*, 2018, **9**, 1235–1240.
38 Y. Yuthavong, B. Tarnchompoo, T. Vilaivan, P. Chitnumsub, S. Kamchonwongpaisan, S. A. Charman, D. N. McLennan, K. L. White, L. Vivas, E. Bongard, C. Thongphanchang, S. Taweechai, J. Vanichtananukul, R. Rattanajak, U. Arwon, P. Fantauzzi, J. Yuvaniyama, W. N. Charman and D. Matthews, *Proc. Natl. Acad. Sci.*, 2012, **109**, 16823–16828.
39 M. V. Papadopoulou, W. D. Bloomer, H. S. Rosenzweig, S. R. Wilkinson, J. Szular and M. Kaiser, *Eur. J. Med. Chem.*, 2016, **117**, 179–186.
40 D. J. Lowes, W. A. Guiguemde, M. C. Connelly, F. Zhu, M. S. Sigal, J. A. Clark, A. S. Lemoff, J. L. Derisi, E. B. Wilson and R. K. Guy, *J. Med. Chem.*, 2011, **54**, 7477–7485.
41 S. Gemma, G. Campiani, S. Butini, G. Kukreja, B. P. Joshi, M. Persico, B. Catalanotti, E. Novellino, E. Fattorusso, V. Nacci, L. Savini, D. Taramelli, N. Basilico, G. Morace, V. Yardley and C. Fattorusso, *J. Med. Chem.*, 2007, **50**, 595–598.
42 A. Rani, J. Legac, P. J. Rosenthal and V. Kumar, *Bioorg. Chem.*, 2019, **88**, 102912.
43 A. Rani, A. Singh, J. Gut, P. J. Rosenthal and V. Kumar, *Eur. J. Med. Chem.*, 2018, **143**, 150–156.

44 M. Sinha, V. R. Dola, P. Agarwal, K. Srivastava, W. Haq, S. K. Puri and S. B. Katti, *Bioorg. Med. Chem.*, 2014, **22**, 3573–3586.
45 C. E. Tranberg, A. Zickgraf, B. N. Giunta, H. Luetjens, H. Figler, L. J. Murphree, R. Falke, H. Fleischer, J. Linden, P. J. Scammells and R. A. Olsson, *J. Med. Chem.*, 2002, **45**, 382–389.
46 N. Walker and D. Stuart, *Acta Crystallogr., Sect. A: Found. Crystallogr.*, 1983, **39**, 158–166.
47 G. M. Sheldrick, *Acta Crystallogr., Sect. C: Struct. Chem.*, 2015, **71**, 3–8.
48 L. J. Farrugia, *J. Appl. Crystallogr.*, 2012, **45**, 849–854.
49 J. M. Coterón, D. Catterick, J. Castro, M. J. Chaparro, B. Díaz, E. Fernández, S. Ferrer, F. J. Gamo, M. Gordo, J. Gut, L. de las Heras, J. Legac, M. Marco, J. Miguel, V. Muñoz, E. Porras, J. C. de la Rosa, J. R. Ruiz, E. Sandoval, P. Ventosa, P. J. Rosenthal and J. M. Fiandor, *J. Med. Chem.*, 2010, **53**, 6129–6152.
50 A. Daina, O. Michielin and V. Zoete, *Sci. Rep.*, 2017, **7**, 42717.
51 L. Guan, H. Yang, Y. Cai, L. Sun, P. Di, W. Li, G. Liu and Y. Tang, *MedChemComm*, 2019, **10**, 148–157.